MASTERARBEIT

Localization of nitric oxide-induced cyclic GMP formation in the vascular wall

zur Erlangung des akademischen Grades

Master of Science

an der Naturwissenschaftlichen Fakultäten der Karl-Franzens-Universität Graz und Technische Universität Graz

(NAWI GRAZ)

vorgelegt von

DI Lea Mihalic

o. Univ.-Prof. Dr. Bernhard-Michael Mayer

Mag. pharm. Dr. rer. nat. Alexander Kollau

Institut für Pharmazeutische Wissenschaften

Graz, Oktober, 2016

Danksagung

Die vorliegende Arbeit wurde in der Zeit von November 2015 bis Juli 2016 am Institut für Pharmazeutische Wissenschaft, Bereich Pharmakologie und Toxikologie, durchgeführt.

Ich danke o. Univ.-Prof. Dr. Bernd Mayer für die Bereitstellung des Themas sowie für die Betreuung.

Weiters danke ich Mag. pharm. Dr. rer. nat. Alexander Kollau für die Betreuung während der praktischen Arbeit, seine Hilfe und Ideen.

Sämtlichen Kolleginnen und Kollegen des Institutes danke ich für die freundliche Aufnahme und die angenehme Atmosphäre.

Table of Contents

1 Introduction

Tunica intima, composed of a monolayer of endothelial cells, is the inner lining of the vasculature and controls vascular function by responding to various hormones, neurotransmitters and vasoactive factors, which affect vasomotion, thrombosis, platelet aggregation and inflammation. The endothelium releases various vasoactive factors, such as nitric oxide (NO), prostacyclin (PGI2) and endothelium derived hyperpolarizing factor (EDHF) as well as vasoconstrictive factors such as thromboxane (TXA2) and endotheliumin-1 (ET-1). The most important mediator of vasodilation in blood vessels is an endothelium-dependent vasodilator NO, which diffuses into the underlying *tunica media* (smooth muscle cells) and triggers a NO/cGMP signalling cascade. [1]

1.1 NO/cGMP signalling cascade

Signal transduction *via* the diatomic radical NO is involved in a number of important physiological processes, including smooth muscle relaxation and neurotransmission. In addition, NO has been shown to play the most important role in the maintenance of basal vasodilator tone of blood vessels. The ability of a blood vessel to dilate is largely dependent upon the activity of the enzyme endothelial nitric oxide synthase (eNOS), which produces NO from the amino acid L-arginine. [2]

eNOS is normally bound to the protein caveolin and is, thus, inactive. eNOS agonists, such as bradykinin (BK), acetylcholine (ACh), adenosine triphosphate (ATP), adenosine diphosphate (ADP), substance P and thrombin [3] activate eNOS through an increase of intracellular calcium (Ca^{2+}) levels by releasing it from the endoplasmic reticulum (ER).

Ca^{2+} forms a complex with calmodulin (CaM), resulting in the dissociation of eNOS from caveolin and its activation. Fig.1. shows a cascade of reactions under an influence of those agonists, which activate a G protein-dependent signalling pathway (Gq proteins), leading to the phospholipase C-dependent hydrolysis of phosphatidylinositol 4,5-biphosphate (PIP_2) that is converted into inositol 1,4,5-triphosphate (IP_3) and diacyl glycerol (DAG). After binding of IP_3 to its receptor on the ER, Ca^{2+} is released into the cytosol and the Ca^{2+}/CaM complex triggers the activation of eNOS. [4] Eventually, eNOS converts L-arginine to NO.

In addition, numerous pathways converge to mobilization of intracellular Ca^{2+}transients providing the eNOS activation *via* CaM. When intracellular Ca^{2+} stores are diminished, the membrane Ca^{2+} channels are opened, allowing extracellular Ca^{2+} to diffuse into the cell. This process of Ca^{2+} regulation is known as store-operated Ca^{2+} entry or capacitive Ca^{2+} entry and is dependent on the levels of intracellular Ca^{2+} in the ER as well as extracellular Ca^{2+}. Alternative mechanism, which regulates NO production, is phosphorylation of a serine residue that occurs *via* shear stress by the actions of protein kinase B (Akt) or by protein kinase A. [1]

However, once NO is produced, it diffuses from the endothelial cells into the adjacent smooth muscle layer [5], where it binds to an HNOX (haem-containing NO/oxygen-binding) domain of the β subunit of the enzyme soluble guanylyl cyclase (sGC), and thus activates the C-terminal cyclase domain. sGC is composed of two homologous subunits, α1 and β1, but only the β subunit binds haem; the corresponding region of the α subunit may have a similar structure, but lacks critical haem-binding residues. The C-terminal domains of both subunits have to be combined to form a heterodimeric catalytic domain (active site). Ligand binding and catalysis require the precise alignment of residues from both subunits; this is very sensitive to relative motion of the subunits as well as to local changes, which underlie the modes of allosteric regulation. [6]

Binding of NO to the haem moiety of the sGC induces its capacity to synthesize the second messenger guanosine 3',5'-cyclic monophosphate (cGMP). Cellular proteins that are directly targeted by cGMP and participate in cGMP signalling include protein kinase G (PKG). (Figure 1)

The biokinetics of cGMP is characterized by three distinct processes: synthesis by sGC, conversion of cGMP to GMP (breakdown) by cyclic nucleotide phosphodiesterases (PDEs) and the excretion of unchanged cGMP by transport proteins in the cell membrane (efflux). [7]

The NO/cGMP/PKG pathway plays a critical role in mediating smooth muscle relaxation, because it is involved in modulating intracellular Ca^{2+}concentration:

- G-protein-activated phospholipase C (PLC-beta) catalyses the hydrolysis of PIP_2 to generate DAG and IP_3, leading to the activation of protein kinase C and the mobilization of intracellular Ca^{2+}. PKG can directly phosphorylate (PLC-beta), leading to inhibition of PLC-beta activity.[8]
- NO/cGMP/PKG signalling promotes increased sequestration and decreased release of Ca^{2+} from intracellular stores as a result of phosphorylation of IP_3 receptor (IP_3R) - associated cGMP kinase substrate (IRAG), which down-regulates the IP_3 receptor and therefore IP_3-mediated Ca^{2+} release from intracellular stores (SR).[9]
- Moreover, the contractile state of smooth muscle is largely determined by the balance between the myosin light-chain kinase (MLCK) and myosin light-chain phosphatase (MLCP) activities. MLCK phosphorylates myosin light chain (MLC) at Ser-19, which leads to increased myosin ATPase activity and muscle contraction. The activity of MLCK is enhanced by increased intracellular Ca^{2+} level, leading to increased formation of the Ca^{2+}/CaM complex that activates MLCK. On the contrary, MLCP reverses this by catalysing the dephosphorylation of the MLC. When the Ca^{2+} concentration is lowered as a result of increased intracellular sequestration and/or efflux, the

kinase is less active, thereby favouring smooth muscle relaxation. In addition, PKG phosphorylates RhoA, resulting in blocking Rho-associated protein kinases (ROCK), which leads to activation of MLCP and reducing phosphorylation of MLC. All these events result in vasorelaxation and reduction in peripheral vascular resistance. [7]

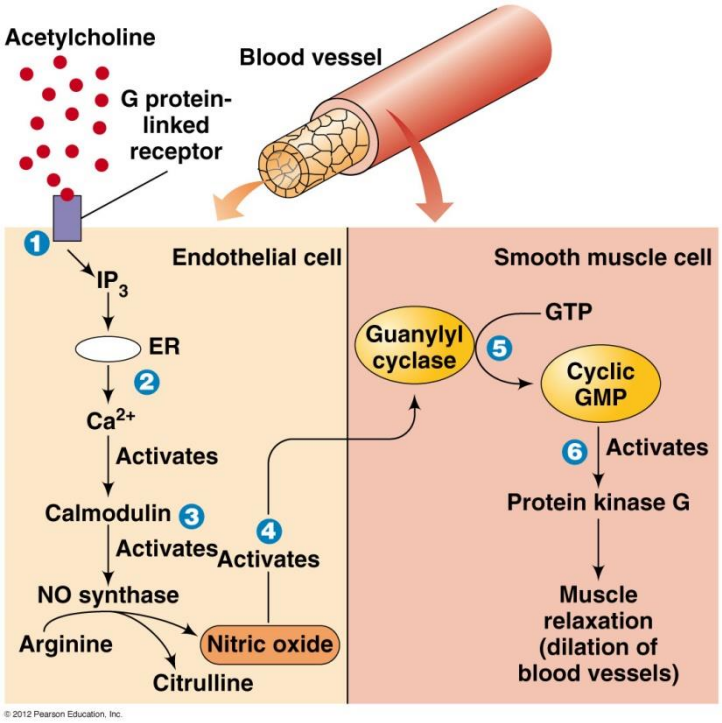

Figure 1: Nitric oxide couples G protein-linked receptor stimulation in endotheliumial cells to relaxation of smooth muscle cells in blood vessels. NO synthase converts arginine to citrulline and NO. The binding of acetylcholine causes the release of NO in vascular endotheliumial cells that causes the relaxation of the vascular smooth muscle (vasodialaton). 1) Binding of acetylcholine to G protein receptors causes IP3 production. 2) IP3 releases calcium ions from endoplasmic reticulum. 3) Ca^{2+} ions and calmodulin form complex which stimulates NO synthase leading to production of NO. 4) NO diffuses from endotheliumial cell into adjacent smooth muscle cells. 5) In smooth muscle cells, NO activates guanylyl cyclase leading to formation of cyclic GMP (cGMP). 6) cGMP activates protein kinase G which phosphorylates several muscle proteins to induce muscle relaxation. (http://www.mun.ca/biology/desmid/brian/BIOL2060/BIOL2060-14/14_14A.jpg)

1.2 The pharmacology of nitroglycerin

According to National Health Service (NHS), 2014, ishemic heart disease (IHD) is the leading cause of death both in the UK and worldwide. It is responsible for more than 73.000 deaths in the UK each year. About 1 in 6 men and 1 in 10 women die from IHD. [10] One of the symptoms of IHD is chest pain or ischemia. Myocardial ischemia occurs when myocardial O_2 supply and demand are imbalanced; thus, the coronary blood flow cannot fully meet the O_2 needs of the heart. The imbalance between oxygen delivery and utilization may result from exertion, from a spasm of the vascular smooth muscle, or from the obstruction of blood vessels caused by atherosclerosis. [11]

A common treatment of angina pectoris is the administration of organic-nitrates, Ca^{2+} channel blockers and β-blockers. [12]. Nitroglycerin (glyceryl trinitrate; GTN) is commonly prescribed short-acting anti-anginal agent that belongs to the organic nitrates or nitro vasodilators (along with sodium nitroprusside and the sydnonimine SIN-1). It has been used clinically since the late 19^{th} century for the treatment of coronary artery disease (CAD), angina pectoris, pulmonary arterial hypertension, congestive heart failure and myocardial infarction. [13]

It is common to apply organic-nitrates either sublingually, orally or *via* transdermal patches. The beneficial clinical effects of GTN are the dilation of large coronary arteries and the reduction of systolic blood pressure, resulting in improved blood supply to the heart and venodilation, resulting in increased venous pooling and the consequent reduction of venous return and cardiac preload. Consequently, the left ventricle pressure myocardial preload and afterload are reduced, thus relieving the heart. [14]

In contrast to sodium nitroprusside or SIN-1, GTN and other organic nitrates do not activate sGC in cell-free systems, but function as prodrugs that must first be bioactivated to produce the active metabolite NO. However, the exact mechanism

by which GTN is metabolized to NO is still not fully understood. Thus, further research is needed, in particular in *in vivo* studies to include the potential involvement of all vascular substructures (e.g. endothelium, smooth muscle). [15]

1.3 ALDH2 dependent bioactivation of GTN

The enzyme ALDH2, belongs to the family of aldehyde dehydrogenases (ALDHs) that catalyse the oxidation of aliphatic and aromatic aldehydes to the corresponding carboxylic acids with $NAD(P)^+$ serving as the electron accepting co-factor. [16]

In 2002, Chen et al. have reported on the bioactivation of GTN by ALDH2, which showed that this enzyme catalyses the formation of 1,2-glyceryl dinitrate (1,2-GDN) and nitrite (NO_2^-) – denitration from low concentrations of GTN and represents the main route of the ALDH2-catalysed reaction (95%). The reaction requires DTT (dithiothreitol) or 2-mercaptoethanol as reductants and is stimulated by the ALDH cofactor NAD^+. [17]

It was proposed that mechanism for GTN denitration involves the esterase activity of ALDH2, i.e. the nucleophilic attack of a nitro group of GTN at Cys-302, resulting in the formation of a thionitrate intermediate and the release of the 1,2-GDN. The thionitrate intermediate would then release nitrite either through the nucleophilic attack of one of the adjacent cysteine residues (Cys-301 or Cys-303), resulting in the formation of a disulfide in the active site, or through Glu-268-aided hydrolysis yielding a sulfenic acid derivative of Cys-302, which could undergo S-thiolation to form a cysteinyl disulfide with one of the adjacent cysteine residues. [18]

On the other hand, in 2005, Kollau and co-workers proposed ALDH2 as the key enzyme that catalyses GTN bioactivation, where NO is directly produced from GTN (5%). [19] There is general agreement that this pathway is essentially involved in GTN-induced relaxation in rodent and human blood vessels, which was confirmed by

studies using a variety of ALDH2 inhibitors, including non-selective compounds, such as chloral hydrate and cyanimide, the ALDH2-selective inhibitors daidzin, and diphenyleneiodonium (DPI). Since comparable results were obtained with blood vessels from several rodent species (mouse, rat, guinea pig) as well as with human arteries and veins, the ALDH2 response is broadly viewed as a general principle of GTN bioactivation in mammalian vascular tissue. [20]

1.4 ALDH2 Inactivation and nitrate tolerance

Nitrate tolerance is defined as an attenuation or even loss of hemodynamic and anti-ischemic effects during continuous nitrate medication. There are several hypotheses to explain the development of nitrate tolerance. In 1995 it was proposed that nitrate tolerance may be associated with increased vascular superoxide production, limiting NO bioavailability due to rapid formation of peroxynitrite, a potent cellular oxidant that may further worsen oxidative stress and endothelial dysfunction. [21] Another potential site of superoxide production is the mitochondrial respiratory chain. Biotransformation of GTN by ALDH2 releases NO, causing reversible inhibition of cytochrome c oxidase. Moreover, respiratory complexes are inhibited by reactive nitrogen species, in particular peroxynitrite and S-nitrosothiols, enhancing mitochondrial superoxide production by uncoupling of the electron transport chain. [22]

Many studies have demonstrated protection against tolerance development by co-administration of antioxidants, such as ascorbate (vitamin C) in laboratory animals [23] and humans. [24] Other antioxidants have also been reported to protect against nitrate tolerance, including the β-adrenergic antagonist carvedilol [25], the vasodilator hydralazine [26] and statins [27].

Another hypothesis for nitrate tolerance is time-dependent inactivation of both the dehydrogenase and esterase activities of ALDH2 by GTN. In the ALDH2 dependent bioactivation of GTN to 1,2-GDN and nitrite, the vicinal thiol groups of cysteine residues in the active site of the ALDH2 act as sulfhydryl reactants, which are oxidized to the corresponding disulphide bridge, resulting in ALDH2 turnover (oxidative inactivation). As this mechanism implicates the essential requirement of reductant for sustained catalysis, it is conceivable that prolonged GTN biotransformation causes depletion of these reductants, resulting in vascular GTN tolerance due to oxidative inactivation of ALDH2. [28]

Moreover, the activity of the GTN-inactivated enzyme, ALDH2, was only partially restored by these reductants, suggesting a significant irreversible component of ALDH2 inactivation. It has been showed that the enzyme converts GTN to NO in a reaction that is independent of GTN bioactivation (clearance-based mechanism), yielding the weakly vasoactive nitrite ion (NO_2^-) and 1,3-GDN. [13]

Nitrate tolerance develops rapidly. Blood vessels become desensitized to vasodilation and it is necessary to provide a daily nitrate-free interval to restore sensitivity to the drug. Stable angina patients avoid nitrate tolerance with an intermittent dose of the drugs, for example, the overnight removal of GTN patches. Therefore, this represents one of the main disadvantages of nitrate therapy. [11]

1.5 ALDH2-independent bioactivation of GTN

Interestingly, in an early study, Horowitz and co-workers showed that diphenyleneiodonium (DPI), which they recently characterized it as a potent ALDH2 inhibitor [29], does not affect the GTN-derived relaxation of porcine coronary arteries, suggesting another, so far unknown ALDH2-independent mechanism of GTN-induced relaxation. In view of current knowledge this observation is surprising

and hard to reconcile with the ALDH2 hypothesis of GTN bioactivation. Our laboratory explained this astounding observation as a consequence of low ALDH2 expression and GTN denitration activity in several types of porcine coronary vessels and in bovine coronary arteries in comparison with rat aortas. [20]

Since NO-activation of sGC plays a major role in vasodilation, ODQ-[1H-[1,2,4]oxadiazolo-[4, 3-a]quinoxalin-1-one] as a typical specific inhibitor for sGC, was used to identify a role of sGC in signal transduction events. ODQ causes oxidation of ferrous sGC, resulting in a shift from 431 to 392 nm, which decreases NO-stimulated sGC activity. [30] Virtually complete inhibition of GTN-induced relaxation by ODQ indicates that vasodilation was caused by activation of sGC. [20]

Considering that GTN does not activate sGC directly, relaxation apparently involves an enzymatic or non-enzymatic reaction, yielding a NO like bioactive species. However, it has been shown previously that ALDH2-catalyzed NO formation (GTN bioactivation) accounts for only about 5% of complete GTN turnover. [31] Thus, low rates of denitration could be accompanied by higher rates of bioactivation in a pathway of GTN denitration that yields stoichiometric amounts of 1,2-GDN and NO or a related sGC activators. It has also been shown that neither the activation of endothelial synthase of NO by GTN itself nor the low affinity effects of GTN in ALDH2-knockout mice can explain GTN bioactivity in porcine vessels. [20]

Taken together, these results provide evidence for a productive and potent ALDH2-independent pathway of GTN bioactivation in porcine coronary arteries. If present in human blood vessels, this pathway could contribute to the therapeutic action of organic nitrates that are not metabolized by ALDH2, e.g. ISMN and ISDN.

1.6 Aims

It was the aim of my master thesis to investigate GTN bioactivation in porcine blood vessels. Therefore, experiments dealing with GTN-stimulated cGMP formation in porcine blood vessels and their substructures (i.e. *tunica intima*, *tunica media*, and *tunica adventitia*) were planned. As very low cGMP levels were noted in porcine blood vessels, porcine cultured smooth muscle cells were also included in experiments. In addition, Western blot analysis was performed to detect possible differences in the distribution of sGC in cytosolic homogenates of substructures of porcine aorta.

2 Material and Methods

Unless stated otherwise all chemicals were from SIGMA Aldrich (Vienna, Austria).

2.1 Cell Culture

Solutions

- **Phosphate-buffered saline (PBS), wash buffer**

NaCl	8.00 g
KCl	0.20 g
Na_2HPO_4	1.44 g
KH_2PO_4	0.20 g

In 1L miliQ-water

- **Dulbecco´s modified Eagle´s culture medium (DMEM)**

DMEM	173.8 g (one package)
$NaHCO_3$	37.0 g
Penicillin/Streptomycin	100.0 mL
Amphothericin B	50.0 mL

In 10 L miliQ-water

pH 7.3

DMEM was supplemented with 10% (v/v) heat-inactivated fetal calf serum (FCS).

The freeze medium contained 20% FCS and 5% DMSO.

- **Trypsin solution**

Trypsin	0.05 %
EDTA	0.02 %
Dissolved in PBS	

2.1.1 Isolation and culture of porcine smooth muscle cells (SMC)

Porcine aortas were obtained from a local abattoir and immediately transported to the laboratory. They were cut open longitudinally using forceps and scissors, and the *tunica media* (smooth muscle cell layer) was peeled off and separated from the other layers. The *tunica media* was cut into small pieces and placed in petri dishes containing the DMEM culture medium supplemented with 10 % (v/v) heat-inactivated FCS. The culture medium was changed every three days. Over time, smooth muscle cells migrated from the tissue pieces into the medium and settled at the bottom of the petri dishes. The aortic tissue was then removed from the dishes. The primary smooth muscle cell cultures were confluent one month after preparation and were then passaged further.

To passage the cells, they were washed twice with PBS, detached from the petri dish using a trypsin solution and then transferred into a 50 mL tube and centrifuged at 1000 rpm at room temperature for 5 min. The supernatant was discarded, the pellet resuspended in 24 mL of fresh medium (DMEM+10 % FCS) and seeded onto a 24 well plate (1 mL resuspended cells per well). Cell spreading was monitored under a microscope. Confluence was reached after 3 days at 37 °C of incubation. Confluent cells were used for the determination of cGMP formation upon incubation with DEA/NO or GTN. (See below)

2.2 Determination of cGMP formation

Solutions

- **3-isobutyl-1-methylxanthin (IBMX) buffer, 1 mM**

3-isobutyl-1-methylxanthin (IBMX)	11.1 mg
Indometacin (1 mM)	50.0 µL

  In 50 mL **TRIS-buffer**, warmed on 37 °C

  Tris hydroxymethyl-aminomethan (TRIS-buffer), incubation buffer

  TRIS stock solution, 500 mM:

Tris hydroxymethyl-aminomethan (TRIS)	60.54 g
NaCl	58.44 g
KCl	3.72 g

  In 1 L miliQ-water

$CaCl_2$ solution	39.8 mM
$MgCl_2$ solution	21.4 mM

  Working solutions were prepared from 50 mL TRIS-stock solution, 50 mL $CaCl_2$, 50 mL $MgCl_2$ and filled up to 500 mL with miliQ-water.

- **2,2-diethyl-1-nitroso-oxyhydrazin (DEA/NO)**

  DEA/NO was from Enzo Life Sciences (Lausen, Switzerland) purchased through Eubio (Vienna, Austria). It was dissolved and diluted in 10 mM NaOH.

  Stock solution 10 mM: 2.06 mg/mL in 10mM NaOH

- **Glyceroltrinitrat/nitroglycerin (GTN)**

  NitroPOHL^R ampules were purchased from a local pharmacy. They contained 1 mg/mL GTN in isotonic glucose, which is equal to 4.4 mM.

Porcine confluent cells grown on 24 well plates were washed and pre-incubated with IBMX buffer for 15 min at 37 °C.

Reactions were started by the addition of DEA/NO (10 nM - 300 µM) or GTN (100 nM - 1 mM) and terminated after 10 min by removal of the incubation medium and addition of 10 mM HCl. Control wells were used for determination of basal cGMP formation. Within 1 hour, intracellular cGMP was released into supernatant and measured by radioimmunoassay.

2.3 Tissue preparation

Porcine hearts and aortas were obtained from a local abattoir and immediately transported to the laboratory. The right coronary artery was carefully explanted, cleaned and washed in ice cold PBS. For the organ bath experiments the coronary artery was cut into app. 5 mm length rings and dry weighted. The *tunica media* (smooth muscle layer) from the porcine aorta was isolated as described in paragraph 2.1.1 and cut into app. 1x1 cm squares washed in PBS buffer and weighted. Four different aortas were prepared as described and used for organ baths for incubation with GTN or DEA/NO.

2.4 Determination of cGMP formation in tissue

Solutions

- **Phosphate-buffered saline (PBS)**

  137 mM NaCl, 2.7 mM KCl, 10 mM Na_2HPO_4, 1.8 mM KH_2PO_4, pH 7.4

- **Krebs-Henseleit buffer**

  Solution 1:

  NaCl 118.40 mM

KCl	5.01 mM
KH_2PO_4	1.20 mM
Solution 2:	
$CaCl_2$	2.5 mM
Solution 3:	
$MgCl_2$	1.2 mM

1 L stock solution:	
50 mL each solution 1,2,3	
D-Glucose	2.0 g
$NaHCO_3$	2.1 g
With distilled water at 1 L, pH 7.4	

The coronary artery rings and *tunica-media* pieces were placed in organ baths containing 3 mL of oxygenated Krebs-Henseleit buffer warmed to 37 ˚C. After 10 min of pre-incubation, GTN (100 nM - 1 mM) or DEA/NO (10 nM - 300 µM) was added and the tissue pieces were incubated for 5 min. The incubated tissue was quickly shock frozen with liquid nitrogen and homogenized in 5 % trichloroacetic acid (TCA) using a dismembrator. These crude homogenates were centrifuged at room temperature for 10 min at 15,000 x g. The supernatants were transferred into eppendorf-tubes and washed 3 times by shaking with diethyl ether for 10 min. After removing the organic phase, samples were analysed for cGMP by RIA immunoassay.

2.5 Radioimmunoassay (RIA)

Solutions

- **Acetate buffer**

$NaCH_3COO$	13.68 g
In 1 L water, pH 4.75	

- **γ-globulin solution**

  5 mg/mL in acetate buffer

- **cGMP – standard solution**

  The following cGMP concentrations were used as standards (fmol / 0.1 mL):

  6.25; 12.5; 25.0 50.0; 100.0; 200.0; 400.0; 800.0

- **Acetylation reagent**

  2 parts of trimethylamine

  1 part of acetanhydride

- **Radioactive antigen (^{125}I-cGMP)**

  ^{125}I-cGMP-tyrosine-methyl-ester was resuspended in acetate buffer/n-propanol (1:1)

  (50 µL solution comply 12,000 cpm)

- **cGMP-antibody**

  anti-cGMP-antibody-serum from rabbit (Sigma), diluted on 20 µL/10 ml 13.8 g/L acetate buffer

The samples were diluted with 10 mM HCl (end volume 230 µL) and acetylated with 10 µL of acetylation reagent. After 30 min, 100 µL of γ-globulin solution, 50 µL of antibody and 50 µL ^{125}I-cGMP were added to 100 µL acetylated sample, vigorously mixed and incubated for 16-20 hours at 4 °C.

Proteins (γ-globulin, Ag/Ab-complex) were precipitated with 1 mL of ethanol and sedimented by centrifugation at 3,660 x g (4 °C). The supernatant was discarded, and radioactivity in the pellet was measured with a γ-counter. The quantification of cGMP was performed using the dilution series of cGMP standards.

2.6 Preparation of cytosols for Western Blot

Solutions

- **Phosphate-buffered saline (PBS)**

  pH 7.4, 137 mM NaCl, 2.7 mM KCl, 10 mM Na_2HPO_4, 1.8 mM KH_2PO_4

- **10mM TRIS buffer**

  pH 7.4, 125 mM KCl, 5 mM EGTA and 2 mM $MgCl_2$

The right coronary artery was carefully explanted, cleaned and washed in ice cold PBS. The tissue was cut into small pieces and homogenized in ice cold 10mM Tris buffer, using a glass-teflon Potter-Elvehjem homogenizer. Homogenates were ultra-centrifuged at 100,000 x g for 1.5 hours. The supernatants were transferred into 1.5 mL eppendorf-tubes and regarded as cytosolic preparations.

The porcine aortas were cleaned of surrounding tissue (e.g. fat tissue) and cut open longitudinally. The *tunica media* (smooth muscle cell layer), *tunica intima* (endothelium and basal lamina), and *tunica adventitia* (outermost connective tissue) were separated by peeling off the respective layer using forceps. Cytosolic preparations of the separated layers and complete aortas were obtained as described above.

Protein concentrations of all preparations were determined with the Pierce BCA ™ Assay Kit (Fischer Scientific Austria GmbH, Vienna, Austria), according to the protocol provided by the manufacturer.

2.7 Western Blot

Solutions

- **Tris-buffered saline with Tween20 (TBST)**

  Stock solution 10 x:

NaCl	80.0 g
Tris base	24.4 g

  Resuspended in 800 mL miliQ-water, pH 7.6

  100 mL stock solution + 900 mL dest. water + 1 mL Tween 20

- **Electrophoresis running buffer**

  Stock solution 5 x:

Tris base	30.2 g
Glycine	188.0 g
Sodium dodecyl sulfate (SDS) 10 %	100.0 mL

  Resuspended in 2 L with miliQ-water, pH 8.4

  200 mL stock solution + 800 mL dest. water

- **Western blot transfer buffer (WBTB)**

  Stock solution 10 x:

Tris base	58.0 g
Glycine	290.0 g

  Resuspended on 2 L miliQ-water, pH 8.4

  700 mL dest. water + 100 mL stock solution + 200 mL methanol (tech.)

- **LaemmLi buffer (2x stock)**

SDS	4 %
Glycerol	20 %
2-mercaptoethanol	10 %
Bromphenol blue	0.004 %

Tris HCl	0.125 M

pH approx. 6.8.

The samples were mixed with the 2x Laemmli buffer (1:1) and heated at 95 °C for 10 min. The denaturated samples (12.5 µg of protein) were separated by sodium dodecyl sulfate polyacrylamide gel electrophoresis (SDS-PAGE) on 10% gels and transferred onto nitrocellulose membranes. The membranes were blocked for 1 hour with 5 % nonfat dry milk in TBST containing 0.05 % Tween 20 (v/v), and then incubated overnight at 4 °C with a primary antibody sGC (alpha1) produced from Prof. Koesling, Bochum against sGC (1:1,000). After incubating the membranes with horseradish peroxidase conjugated anti-rabbit IgG (1:5,000), immunoreactive bands were detected by chemiluminescence using ECL Prime Western Blot Detection Reagent (GE Healthcare, purchased via VWR, Vienna, Austria) and quantified densitometrically using the E.A.S.Y Win 32 Software (Herolab, Vienna, Austria).

2.8 Statistical Analysis

Data shown in our results are expressed as mean values ± SEM, and the number of experiments (n) is given in the corresponding text. Statistical analyse was performed by ANOVA, using Kaleida-Graph Software (version 4.1.3). Significance was assumed at $p < 0.05$.

3 Results

3.1 Formation of cGMP

The formation of cGMP in response to GTN was measured in cultivated porcine smooth muscle cells, in intact porcine coronary arteries and in the *tunica media* (smooth muscle layer) from porcine aortas, to compare the degree of cGMP accumulation in different blood vessels and the contribution of the smooth muscle layers. All experiments were repeated using the NO donor- DEA/NO as positive control.

3.1.1 cGMP formation in cultured porcine smooth muscle cells

cGMP formation was measured in confluent cultured porcine smooth muscle cells, which were incubated with an increasing concentration of DEA/NO or GTN. As shown in Figure 2, DEA/NO has 160 times potentiated the formation of cGMP of that of the basal value. Maximal effect was reached in the presence of 10 µM DEA/NO (160 ± 50 pmol cGMP/10^6 cells) and a half maximal effective concentration (EC_{50}) was found at $5.4x10^{-8}$ M. On contrary, GTN has hardly changed cGMP level and the EC_{50} was approximately $1.7x10^{-5}$ M.

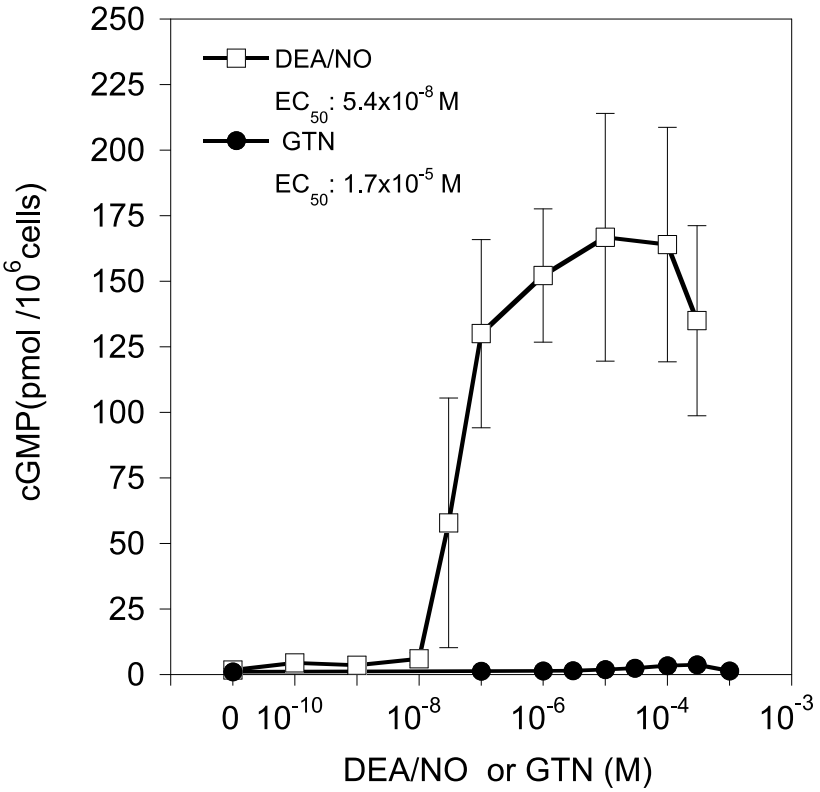

Figure 2: cGMP formation in cultured porcine smooth muscle cells in response to DEA/NO and GTN. Cells were incubated 10 min with increasing concentrations of DEA/NO or GTN. Formation of cGMP was determined by RIA as described under Methods. Data are mean values ± SEM of 3-4 experiments.

3.1.2 DEA/NO stimulated cGMP formation in PCA and in *tunica media*

cGMP level upon DEA/NO incubation was significantly higher in PCA as in *tunica media.* Maximal cGMP level (850 fmol cGMP/mg tissue) was observed in the presence of $3x10^{-4}$ M DEA/NO, with no distinct maximum. At the same DEA/NO concentration, the cGMP level in *tunica media* has already reached the maximum. However, the maximal cGMP level was substantially lower (110 fmol/cGMP/mg tissue).

The EC_{50} in *tunica media* was $1.4x10^{-6}$ M whereas the EC_{50} in PCA was not determined. (Due to the missing maximum).

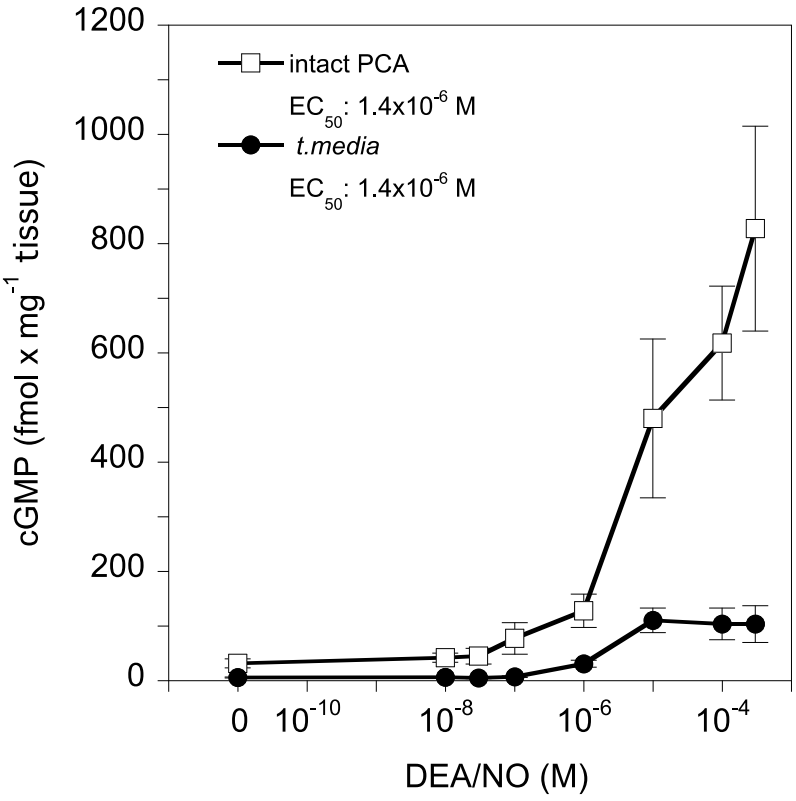

Figure 3: Effect of DEA/NO on the formation of cGMP in intact PCA and *tunica media*. Concentration-response curves to DEA/NO (in range from 10^{-8} to $3x10^{-4}$ M DEA/NO) in PCA and in porcine *tunica media*. Weighted tissue was incubated for 5 min. Response to increasing concentrations of DEA/NO is in the figure present as fmol cGMP/mg tissue, determined by RIA. Data are mean values ± SEM of three individual experiments.

As basal cGMP formation was higher in PCA, the fold-increase was calculated and compared, thus normalizing the results. As shown in Fig. 4 normalized cGMP formation was identical in both tissues at up to $3x10^{-6}$ M DEA/NO. In *t.media,* cGMP increased maximally by approx. 18 times the basal value (at 10^{-5} M DEA/NO), whereas in PCA, the values of cGMP increased maximally by approx. 30 times (at $3x10^{-4}$ M DEA/NO).

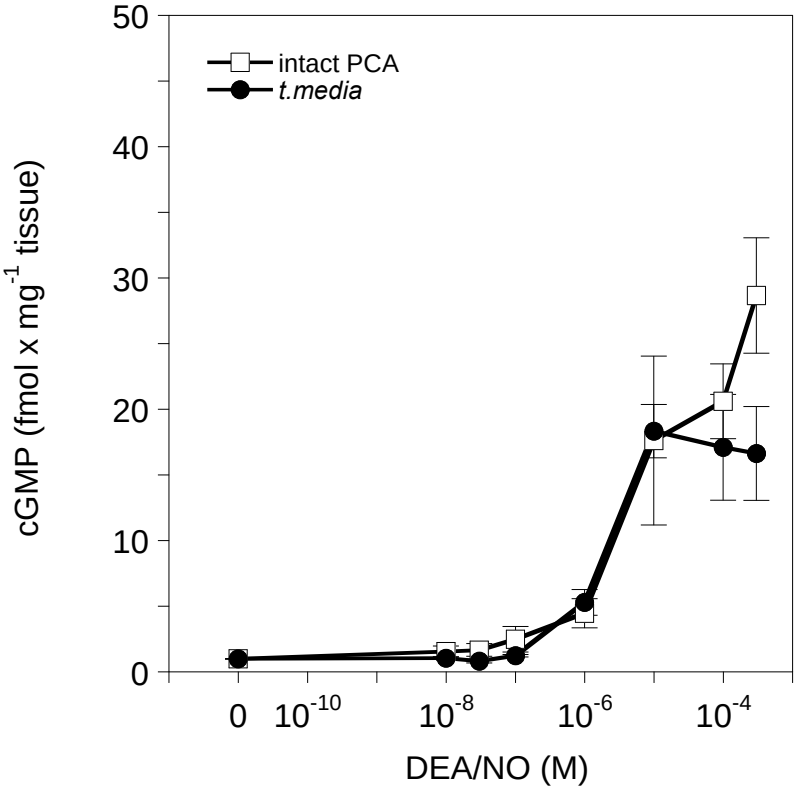

Figure 4: cGMP formation expressed as n-fold of basal value in PCA and in porcine *tunica media* in response to DEA/NO. Data from the concentration-response curves shown in Fig. 3 were normalized to basal values. Data are mean values ± SEM of three individual experiments.

3.1.2.1 GTN-stimulated cGMP formation

The effect of GTN on the formation of cGMP in PCA and in porcine *tunica media* is shown in Figure 5. In PCA, cGMP formation level increased maximally almost 5-fold over basal in the presence of $3x10^{-4}$ M GTN (40 and 183 fmol/mg tissue basal and maximal cGMP level, respectively). The calculated EC_{50} was $5.7x10^{-5}$ M. However, as it was the case for DEA/NO, GTN-stimulated cGMP formation in *tunica media* was substantially lower. In *tunica media*, highest increase of cGMP formation level was found in the presence of 10^{-3} M GTN (29.5 fmol/mg tissue), with no maximum level known. This is equivalent to a 4-fold increase of basal cGMP level in *tunica media*.

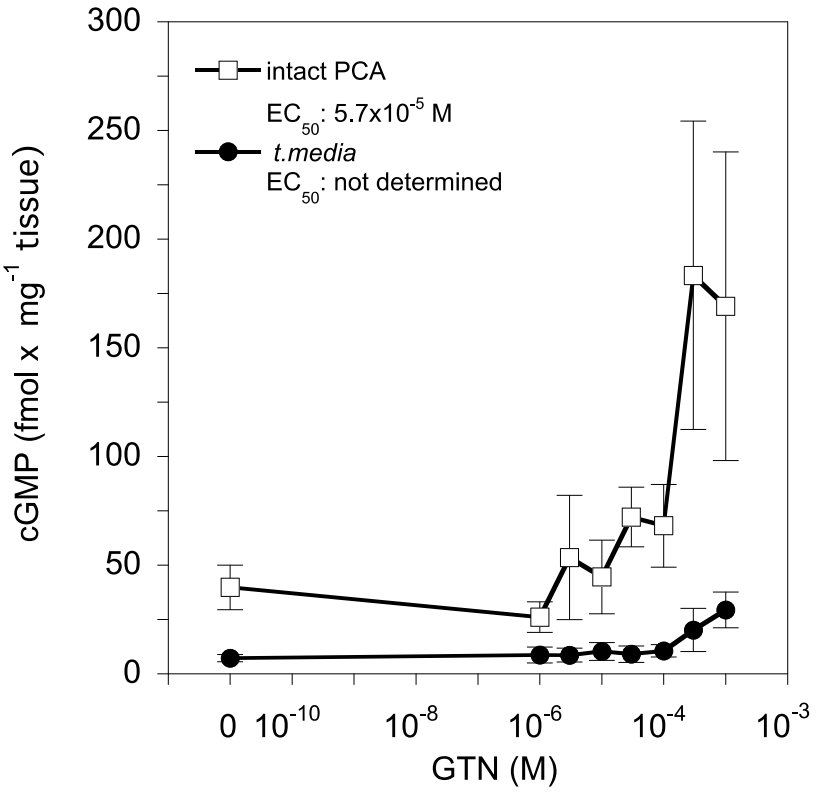

Figure 5: Effects of GTN on the formation of cGMP in intact porcine coronary artery (PCA) and in porcine *tunica media* (smooth muscle cells). Concentration-response curves to GTN (10^{-6}-10^{-3} M) in PCA and in porcine *tunica media* were established. Weighted tissue was incubated for 5 min. Response to increasing concentrations of GTN is denoted as fmol cGMP/mg tissue, which was determined with RIA. Data are mean values ± SEM of three animals.

In this set of experiments, basal cGMP formation level was higher in PCA (cf. Fig 3). Therefore the fold-increase was calculated in order to normalize the results. As shown in Fig. 6 the overall fold increase of cGMP levels was comparable for both tissues. In *t.media,* cGMP increased approximately 5-fold over basal value at $3x10^{-4}$ M GTN, with no maximum known. In PCA, the highest values of cGMP (at $1x10^{-3}$ M GTN) correspond to about 4-fold increase of basal levels.

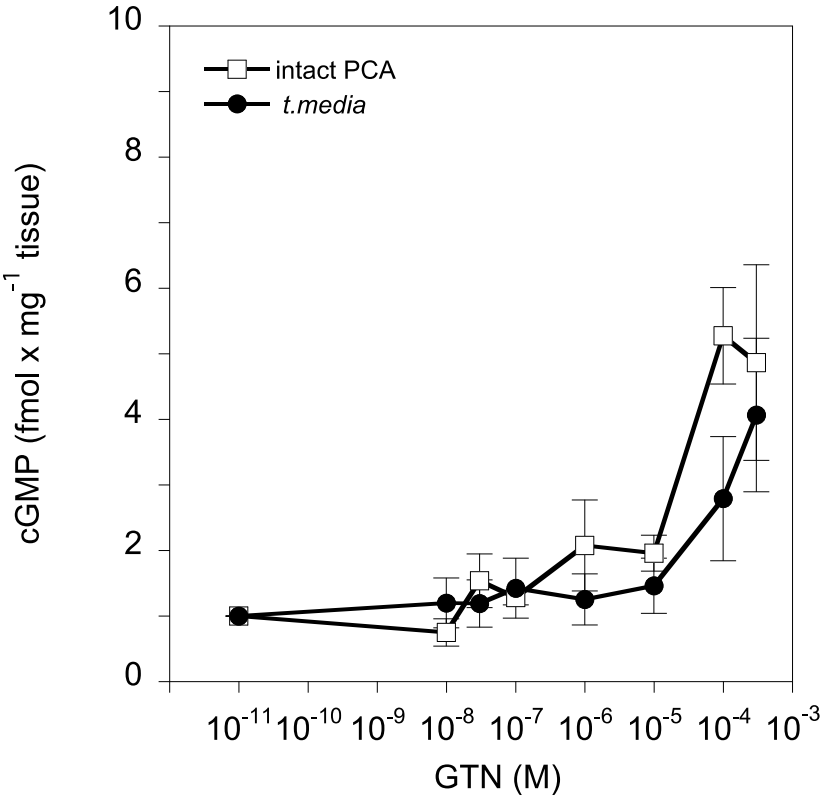

Figure 6: Comparison of cGMP formation in PCA and porcine *tunica media* in response to GTN. Data from concentration-response curves from Fig. 5 are normalized on basal values. Data are mean values ± SEM of three individual experiments.

3.1.3 cGMP formation in the layers of the porcine aorta

Because of the measured low values of cGMP formation in response to DEA/NO in the porcine *tunica media* in comparison to the PCA, the experiment was repeated with several isolated layers of porcine aortic wall in the presence of 10^{-5} M DEA/NO. The experiment was conducted as described in the Methods. As shown in Figure 7, the cGMP formation in the isolated layers was significantly lower than in complete aorta. The untreated tissue yielded 640.4 fmol cGMP/mg tissue whereas the cGMP levels obtained from isolated layers where below 50% of that (177.8, 216.8, and 274.1 fmol cGMP/mg tissue for *t. media, t. media*+endothelium, and *t. adventitia* respectively). Adding up the cGMP formation values of isolated layers give approx. the same cGMP value as it is obtained in intact aorta.

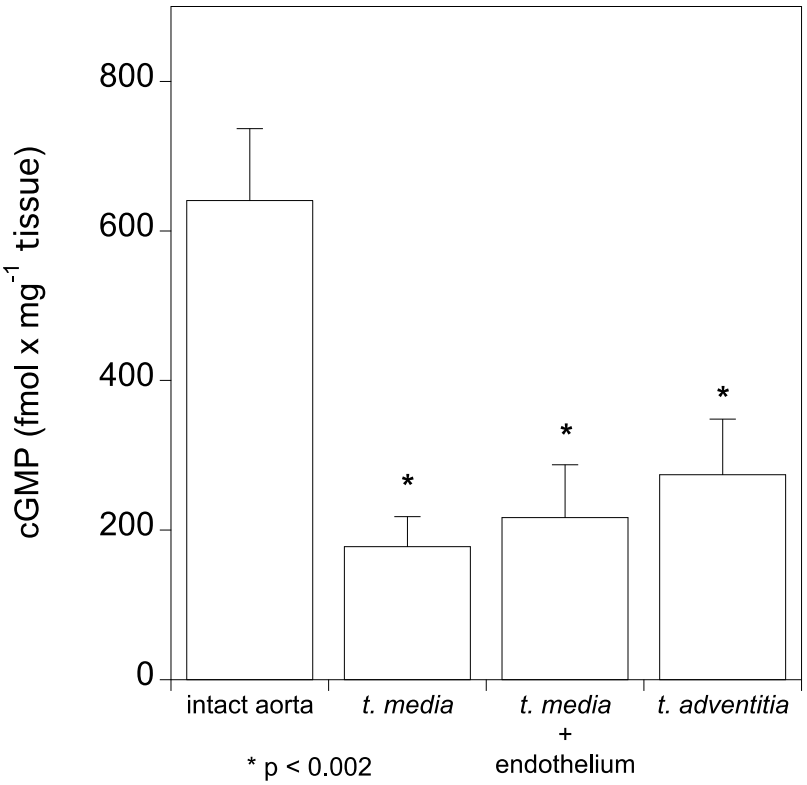

Figure 7: Effects of 10^{-5} M DEA/NO on formation of cGMP in complete aorta (intact), *t.media, t.media*+endothelium, *t.adventitia.* Each layer was carefully isolated and incubated for 5 min in the presence of DEA/NO (10^{-5} M). Formation of cGMP was determined with RIA. Data are mean values ± SEM (expressed as fmol cGMP/mg tissue) of four individual experiments.

3.1.4 The influence of aortic layer separation on cGMP formation

All aortic layers produced comparable amounts of cGMP after incubation with DEA/NO (10^{-5} M). The cGMP response to DEA/NO in the complete aorta was significantly higher. For that reason, we investigated whether mechanical separation of the individual layers affected cGMP formation. The experiment was repeated as described above, except that the tissue homogenates were combined again after incubation and treated as one sample. The results obtained were compared with those obtained from untreated (intact) aortic tissue pieces. cGMP formation level in

the intact porcine aorta was significantly higher than in the recombined layers. The level of cGMP in the intact porcine aorta increased up to 440 fmol cGMP/mg tissue, which is approx. 50 % higher than in separated layers (260 fmol cGMP/mg tissue).

3.2 Quantification of sGC expression in the porcine aorta

To support the findings of stimulated cGMP formation in response to DEA/NO (see Figure 7), we studied sGC expression in the complete porcine aorta and in aortic layers by quantitative immunoblotting, using β-sGC as a standard protein. A representative blot is shown in Figure 9. The same amount (12.5 µg) of cytosolic protein of the complete aorta and isolated layers of the vessel wall were loaded onto each lane. The bold band in each lane at 72 kDa represents β-sGC (upper panel). Clear bands at approx. 37 kDa represent GAPDH, which was used as loading control (lower panel).

In the Figure 9, β-sGC in the cytosolic homogenates of the complete aorta and isolated layers of the vessel wall was quantitative determined and compared within cytosolic homogenates (bold bands at 72 kDa). In intact aorta (IA1-IAl3) 0.57 ± 0.03 ng sGC were found per µg cytosolic protein. The *t.media* preparations (M1-M3) contained 0.58 ± 0.09 ng sGC/µg. In *t.media* + endothelium (M+E1-M+E3) the amount of sGC was 0.64 ± 0.05 ng/µg, and 0.61 ± 0.06 ng of sGC per µg cytosolic protein was found in *t.adventitia* (AD1-AD3).

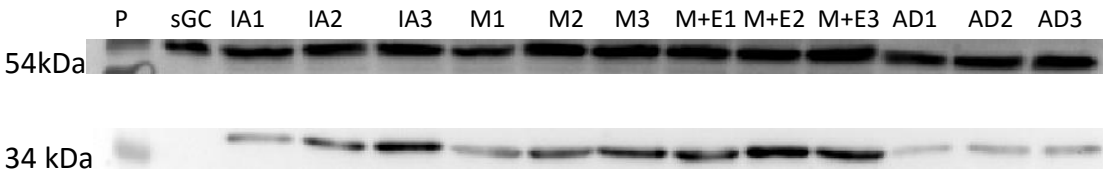

Figure 8: Representative Western blot of aortic cytosols. 12.5 µg of protein of the corresponding preparations was loaded onto each lane and separated by SDS-PAGE. IA1-lA3 represent intact porcine aorta, M1-M3 represent *tunica media,* M+E1-M+E3 represent *tunica media*+endothelium, AD1-AD3 represent *tunica adventitia*. Purified sGC (5 ng) was used as standard for protein quantification. sGC (upper panel) was detected with an anti-sGC antibody (1:1000) resulting in strong bands corresponding to approx. 72 kDa. GAPDH (lower panel) was detected with an anti-GAPDH antibody (1:10,000) resulting in clear bands at approx. 37 kDa.

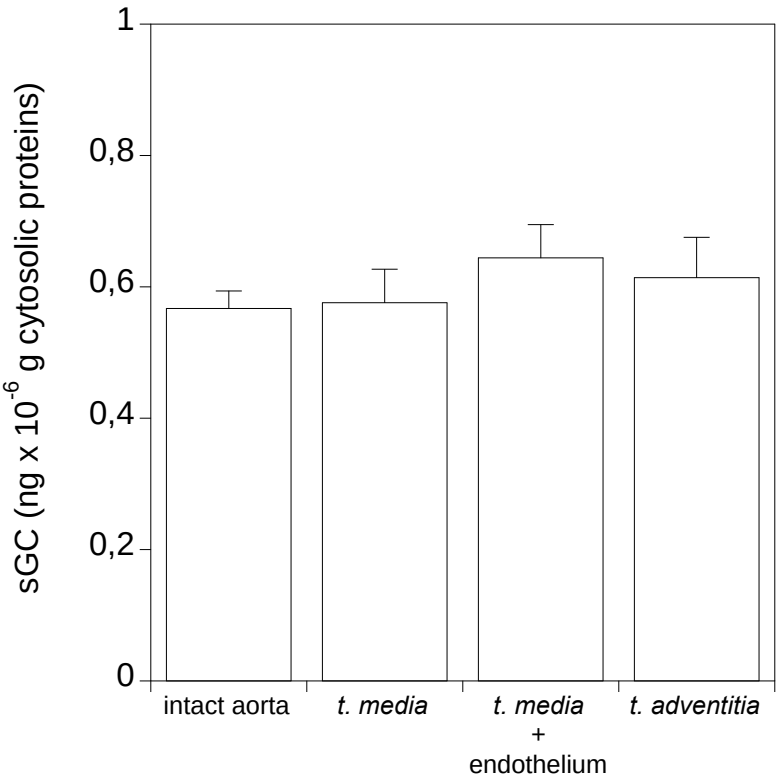

Figure 9: sGC expression in porcine aorta and its substructures. Data are presented as ng sGC per µg cytosolic protein and represent mean values ± SEM of three individual experiments. ANOVA analysis showed no significant differences between all preparations.

4 Discussion

Vasodilation of blood vessels is performed by relaxation of smooth muscle layer, which is mediated by NO/cGMP signalling pathway. [32] NO as the ˝first messenger˝ binds tightly to a prosthetic haem on the β-subunit of sGC and causes a 100-200 fold activation of the enzyme. [5] Activation of NO-sGC increases conversion of GTP to cGMP, resulting in elevation of cGMP, which initiates the cGMP-signalling pathway and thus the relaxation of the blood vessels. [33] NO is released through a bioactivation process from a number of nitrovasodilators, such as GTN. In recent years, a great deal of evidence has been produced that supports the view that clinically relevant denitration of GTN to produce 1,2-GDN and NO_2^- is catalysed by ALDH2.

ALDH2-dependent GTN bioactivation appears to be the main principle of GTN-mediated relaxation of mammalian vascular tissue (mouse, rat, guinea pig as well as human arteries) [34], but not in bovine coronary arteries. [35] Interestingly, the study performed by a group in our laboratory explained this observation as a consequence of low ALDH2 expression in bovine and porcine coronary arteries, where the protein was hardly detectable. A similar pattern was observed for the rates of denitration, which were high in rat aorta and very low in porcine coronaries. It was also confirmed [20] that vasodilation is caused by the activation of sGC, which is not directly activated by GTN. Until now, several enzymes, instead of ALDH2, have been considered as potential candidates to catalyse the conversion of GTN, such as ALDH3A1, cytochrome P450 and GSH transferase, but all were excluded. The activation of endothelial NO synthase by GTN itself [36], which was considered as an alternative explanation for GTN bioactivity, was neither involved. So, it appears that GTN is bioactivated in porcine and bovine blood vessels through an unknown ALDH2-independent pathway. [20]

The initial aim of this Master thesis was to investigate this ALDH2-independent GTN bioactivation in porcine smooth muscle.

Because vasodilation is performed through NO-sGC pathway, yielding cGMP in smooth muscle cells, we wanted to characterise the formation of cGMP in the porcine vasculature (using cultured smooth muscle cells, aortic *t.media* and an intact coronary artery) by GTN and DEA/NO.

The present data confirm the study, done in our laboratory [20] that GTN conversion to NO is not the main pathway involved in formation of cGMP in the porcine vasculature. GTN incubation of the samples produced only 4-5 fold increase in basal cGMP formation (Fig. 2, 5). As reported in 1985 [37], we wanted to confirm that in smooth muscle layer the most cGMP is produced. Therefore we made cGMP assays with GTN incubation of *t.media* as well as the PCA. In *t.media,* cGMP increased approx. 5 fold over basal at $3x10^{-4}$ M GTN, with no maximum known. In PCA, the cGMP increased approx. 4 fold over basal (maximum) when incubated with 10^{-3} M GTN. In addition, a higher GTN concentration of up to $3x10^{-4}$ M caused an increase in cGMP formation, but by higher concentration, cGMP formation decreased. From the present results it can be observed that GTN only barely stimulated cGMP formation in all samples. Thus, GTN was no longer our subject of investigation.

On the other hand, stimulation with DEA/NO led to an 18-30-fold increase in basal cGMP formation (Fig. 2, 3, 4). It is not surprising that DEA/NO incubation led to a much higher level of cGMP formation than GTN, which confers that NO is an activator of sGC, which is responsible for cGMP formation. Confirming that stimulation of cGMP formation with DEA/NO takes place in *t.media*, a cGMP assay was performed again for PCA as well *t.media*. Figures 3, 4 show that in PCA, cGMP formation level was significantly higher (850 fmol cGMP/mg tissue at $3x10^{-4}$ M DEA/NO, with EC_{50} by $1.4x10^{-6}$ M) than in *t.media* (110 fmol/ cGMP/mg tissue at $3x10^{-4}$ M DEA/NO, with EC_{50} by $1.4x10^{-6}$ M), which was definitely not expected. The

highest cGMP level by PCA was observed at $3x10^{-4}$ M DEA/NO, whereas in *t.media* the maxiumum was already present at the same concentration.

These results were confirmed with porcine cultured smooth muscle cells, shown in Figure 2. DEA/NO incubation led to 160-fold increase in the basal cGMP formation level with a maximum (160 ± 50 pmol cGMP/ 10^6 cells at 10 µM DEA/NO) and EC_{50} at $5.4x10^{-8}$ M. Incubating with GTN hardly changed the cGMP formation level, and the EC_{50} was at $1.7x10^{-5}$ M, which confirms previous PCA and *t.media* results. Relying on these results, we came to the question of how porcine vasculature relaxes, if there is a negligible amount of cGMP formed under the GTN stimulation. Because NO is not the metabolite in GTN bioactivation, we wanted to take a look at NO's influence on the formation of cGMP, and which layer of the porcine aorta it is most effective in.

For that purpose we dissected other porcine aortic layers (*t.media*, *t.media*+endothelium, *t.adventitia)* and repeated the experiment with DEA/NO. After being incubated with the 10^{-5} M DEA/NO, cGMP formation level was approx. the same in all layers (*t.media*, *t.media* + endothelium, *t.adventitia)* and was significant to the intact aorta, which was definitely not expected (Fig. 7). Because cGMP conversion is dependent on NO-sGC activation, it was expected that by adding exogenous NO, the most cGMP formed would be present in *t.media* + endothelium, since endogenous NO is produced in the endothelium by eNOS synthase. It is also surprising that the response to DEA/NO in *t.adventitia* appears to be as big as in *t.media*, although cGMP synthesis seems to be located in smooth muscle cells. Since *t.media* is the thickest layer in the aorta, it was expected that the similar amounts of cGMP per weight of *t.media*+endothelium is also formed in accordance with the weight of intact an aorta.

In addition, sGC distribution was compared in intact aorta and in smooth muscle layer. (Fig.9). Thus, we investigated whether the act of isolating the layers might be responsible for this unexpected result. To do so, the aortic layers were separated and incubated individually at first, but recombined before cGMP level

determination. If cGMP levels would be identical to those of the intact aorta, the previously found difference might be due to a methodological problem. Unfortunately, the reunited tissue layers still showed decreased cGMP levels compared to the native aorta. This is clear evidence for the interference in cGMP formation that is caused by the separation of aortic layers. One explanation could be the stress-induced oxidation [38] of sGC during the isolation process. As a reduced (i.e. Fe^{2+}) prosthetic haem group of sGC is essential for NO binding [39], such oxidative stress would certainly decrease the enzyme's response to DEA/NO stimulation. However, this issue was not covered in this thesis and might be the subject of further studies.

Conslusion

Taken together, the results suggest that GTN bioactivation is not the main root of the NO source in porcine coronary arteries, which activates sGC. First of all, there is a main report of a lack of GTN bioactivated-ALDH2 expression [30], and our results have shown that GTN, in comparison to DEA/NO, barely has an impact on the cGMP formation as an indicator of vasorelaxation. Furthermore, it is not only the vascular smooth muscle layer that has an impact on vasorelaxation, but also the other layers. In addition, the results show that aortic layers dissection leads to either the loss of some co-factors that are necessary for vasorelaxation or to the damage of the layers by isolation. Either way, further investigation is necessary in order to avoid these problems in subsequent experiments.

5 Abstrakt

Es ist bekannt, dass GTN-Bioaktivierung ALDH2 abhängig ist (Ratten, Meerschweinchen, sowie menschliche Arterien), wodurch NO gebildet ist, die sGC direkt aktiviert, was zu erhöhter Bildung des sekundären messenger führt, cGMP aus GTP, die für der Vermittlung von Vasorelaxation sorgt. Interessanter weise wurde die ALDH2 Expression kaum in Schweine-Koronararterien nachgewiesen, was auf eine bis jetzt unbekannte ALDH2 unabhängige GTN induzierte Relaxation hinweist [20].

In dieser Studie haben wir gezeigt, dass GTN kaum einen Einfluss auf die Bildung von cGMP in Schweinen Blutgefäß hat. NO ist aber dennoch an diesem Signalweg beteiligt, was durch die Verwendung von kultivierten glatten Schweinezellen bestätigt wurde. Das Vergleich von geringen Mengen an cGMP-Bildung in Schweinen *t.media* und in intakten Schweinen Koronararterie führte uns zur Isolierung anderer Aorten Schichten (*t.media* mit Endothelium und *t.adventitia*), um deren Einfluss auf die Vasorelaxation zu bestimmen. Überraschenderweise wurden alle Aorten-Schichten durch die Zugabe von DEA / NO gleichmäßig an die cGMP-Bildung beteiligt, aber das war immer noch nicht vergleichbar mit der cGMP-Bildung in intakten vollständigen Aorta. Diese Beobachtung war überraschend, da die Vasoelaxation durch glatte Muskelzellen ausgelöst ist, die in *t.media* vorhanden sind. Weiterhin war die cGMP Menge in den Aorten-Schichten, die isoliert wurden und dann vor dem cGMP-Assay erneut verbunden/zusammen gebracht, immer noch viel niedriger als die in der intakten vollständigen Aorta. Dies ist ein klarer Beweis für die Interferenz in cGMP Bildung, die durch die Trennung von Aorten Schichten verursacht wird, jedoch sind weitere Untersuchungen notwendig, um Probleme in den nachfolgenden Experimenten zu vermeiden.

6 Abstract

It is well established that GTN bioactivation is ALDH2 dependent (rats, guinea pig, as well as human arteries), yielding NO, which directly activates sGC, leading to increased formation of the second messenger, cGMP, from GTP, mediating vasorelaxation. Interestingly, it has been shown that ALDH2 expression was hardly detected in porcine coronary arteries, showing other and so far unknown ALDH2 independent GTN-induced relaxation. [20]

In this study, we showed that GTN has barely any effect on the formation of cGMP level in porcine vessels, but NO is still involved in this signalling pathway, which was confirmed using cultured porcine smooth cells. The low amount of cGMP formation in porcine *t.media* in comparison to the intact porcine coronary artery led us to the isolation of other aortic layers (*t.media* with endothelium and *t.adventitia*), to determine their impact on vasorelaxation. Surprisingly, all aortic layers were equally involved in cGMP formation after adding DEA/NO, but that was still not comparable with the cGMP formation in intact complete aorta. This observation was surprising, because vasorelaxation is supposed to be triggered through smooth muscle cells, which are present in *t.media*. Furthermore, the cGMP amount in the aortic layers, which were isolated and then re-joined before the cGMP assay, was still much lower than that in the intact complete aorta. However, this is clear evidence for the interference in cGMP formation that is caused by the separation of aortic layers, and further investigation is necessary in order to avoid these problems in subsequent experiments.

7 Abbreviations

ADP	adenosine diphosphate
ATP	adenosine triphosphate
ACh	acetylcholine
ALDH2	aldehyde dehydrogenase-2
BK	bradykinin
CAD	coronary artery disease
CaM	calmodulin
cGMP	cyclic guanosin monophosphate
DAG	diacyl glycerol
DEA/NO	2,2-diethyl-1-nitroso-oxyhydrazine
DPI	diphenyleneiodonium
EDHF	endothelium derived hyperpolarizing factor
eNOS	endotheliumial NO synthase
ER	endoplasmic reticulum
ET-1	endotheliumin-1
HNOX	haem-containing NO/oxygen-binding domain
IP_3	inositol 1,4,5-triphosphate
IRAG	IP_3 receptor (IP_3R) - associated cGMP kinase substrate

1,2-GDN	1,2-glycerol dinitrate
GTN	glycerol trinitrate
GTP	guanosin triphosphate
IHD	ischemic heart disease
MLC	myosin light chain
MLCK	myosin light chain kinase
MLCP	myosin light chain phosphatase
NAD(P)+	nicotinamide adenine dinucleotide(phosphate), oxidized form
NO	nitric oxide
ODQ	1H-[1,2,4]oxadiazolo-[4, 3-a]quinoxalin-1-one]
PCA	porcine coronary artery
PDE	phosphodiesterase
PGI2	prostacyclin
PIP_2	phosphatidylinositol 4,5-biphosphate
PKG	protein kinase G
ROCK	Rho-associated protein kinase
SEM	standard error of the mean
SDS	sodium dodecyl sulfate
SMC	smooth muscle cell
SR	sarcoplasmic reticulum

sGC	soluble gunylate cyclase
TXA2	thromboxane

8 References

1. A. Sandoo, Jet J. C. S Veldhuijzen van Zanten, G. S. Metsios, D. Carroll and G. D. Kitas. The Endothelium and Its Role in Regulating Vascular Tone. Open Cardiovasc Med J. 4: 302–312 (2010)
2. J. W. Denninger and M. A. Marletta, Guanylate cyclase and the NO/cGMP signaling pathway. Biochim Biophys Acta. 2-3: 334-350 (1999)
3. S. Moncada and E. A. Higgs. The discovery of nitric oxide and its role in vascular biology. B J Pharmacol. 147: 193-201 (2006)
4. D. M. Dudzinski and T. Michel. Life history of eNOS. Cardiovasc research. 75: 247-260 (2007)
5. L. J. Ignarro, R. G. Harbison, K. S. Wood and P. J. Kadowitz. Activation of purified soluble guanylate cyclase by endothelium-derived relaxing factor from intrapulmonary artery and vein: stimulation by acetylcholine, bradykinin and arachidonic acid. J Pharmacol Exp 237: 893-900 (1986)
6. Opher Gileadi. Structures of soluble guanylate cyclase: implications for regulatory mechanisms and drug development. Biochem Soc Trans. 42: 108–113 (2014)
7. S. H. Francis, J. L. Busch, J. D. Corbin and D. Sibley. cGMP-Dependent Protein Kinases and cGMP Phosphodiesterases in Nitric Oxide and cGMP Action. Pharmacol Rev. 62: 525-563 (2010)
8. C. Xia, Z. Bao, C. Yue, B. M. Sanborn and M. Liu. Phosphorylation and regulation of G-protein-activated phospholipase C-beta 3 by cGMP-dependent protein kinases. J Biol Chem. 276: 19770-7 (2001)
9. V. Vanderheyden, B. Devogelaere, L. Missiaen, H. DE Smedt, G. Bultynck and J. B. Parys. Regulation of inositol 1,4,5-trisphosphate-induced Ca2+ release by reversible phosphorylation and dephosphorylation. Biochim Biophys Acta. 1793: 959-970 (2009)
10. National Health Service (NHS), 2014. Coronary heart disease. Available at http://www.nhs.uk/conditions/coronary-heart-disease/pages/introduction.aspx [Accessed 28.09.2016]
11. K. S. Hiwa. Antianginal Drugs Pharmacology. Lippincott illustrated rewiev, Pharmacology. (2013)
12. E. M. Antman. Cardiovascular Therapeutics: A Companion to Braunwald's Heart Disease. 4th edition. Elsevier, Saunders. (2013)

13. B. Mayer and M. Beretta. The enigma of nitroglycerin bioactivation and nitrate tolerance: news, views, and troubles. Br J Pharmacol. 155: 170-184 (2008)
14. S. M. Bode-Böger and G. Kojda. Organic nitrates in cardiovascular disease. Cellular Molecular Biology. 51: 307-320 (2005)
15. H. F. Galley and N. Webster. Physiology of the endothelium. Br J Anaesth. 93: 105-113 (2004)
16. E. Racker. Aldehyde Dehydrogenase, a Diphosphopyridine Nucleotide-linked Enzyme. J Biol Chem. 177: 883-892 (1949)
17. Z. Chen, J. Zhang and J. S. Stamler. Identification of the enzymatic mechanism of nitroglycerin bioactivation. Proc Natl Acad Sci U.S.A. 12: 8306–8311 (2002)
18. S. Biswas, A. S. Chida and I. Rahman. Redox modifications of protein-thiols: emerging roles in cell signaling. Biochem Pharmacol. 71: 551-564 (2006)
19. A. Kollau, A. Hofer, M. Russwurm, D. Koesling, W. M. Keung, K. Schmidt, F. Brunner and B. Mayer. Contribution of aldehyde dehydrogenase to mitochondrial bioactivation of nitroglycerin: evidence for the activation of purified soluble guanylate cyclase through direct formation of nitric oxide. Biochem J. 385: 769–777 (2005)
20. R. Neubauer, G. Wölkart, M. Opelt, C. Schwarzenegger, M. Hofinger, A. Neubauer, A. Kollau, K. Schmidt, A. Schrammel and B. Mayer. Aldehyde dehydrogenase-independent bioactivation of nitroglycerin in porcine and bovine vessels. Biochem Pharmacol. 93: 440-118 (2015)
21. E. Schulz, T. Jansen, P. Wenzel, A. Daiber and T. Münzel. Nitric oxide, tetrahydrobiopterin, oxidative stress, and endotheliumial dysfunction in hypertension. Antiox Redox Signal. 10: 1115–1126 (2008)
22. J. D. Erusalimsky and S. Moncada. Nitric oxide and mitochondrial signaling: from physiology to pathophysiology. Arterioscler Thromb Vasc Biol. 27: 2524–2531 (2007)
23. B. Fink, S. Dikalov and E. Bassenge. A new approach for extracellular spin trapping of nitroglycerin-induced superoxide radicals both in vitro and in vivo. Free Rad Biol Med. 28: 121–128 (2000)
24. G. R. Thomas, J. M. DiFabio, T. Gori and J. D. Parker. Once daily therapy with isosorbide-5-mononitrate causes endotheliumial dysfunction in humans. Evidence of a free radical-mediated mechanism. J Am Coll Cardiol. 49: 1289–1295 (2007)

25. E. El. Demerdash. Evidences for prevention of nitroglycerin tolerance by carvedilol. Pharmacol Res. 53: 380–385 (2006)
26. T. Münzel, S. Kurz, S. Rajagopalan, M. Thoenes, W. R. Berrington, J. A. Thompson, B. A. Freeman and D. G. Harrison. Hydralazine prevents nitroglycerin tolerance by inhibiting activation of a membrane-bound NADH oxidase—a new action for an old drug. J Clin Invest. 98: 1465–1470 (1996)
27. A. Otto, D. Fontaine, J. Fontaine and G. Berkenboom. Rosuvastatin treatment protects against nitrate-induced oxidative stress. J Cardiovasc Pharmacol. 46: 177–184 (2005)
28. M. V. Wenzl, M. Beretta, A. C. Gorren, A. Zeller, P. K Baral, K. Gruber, M. Russwurm, D. Koesling, K. Schmidt, B. Mayer. Role of the general base Glu-268 in nitroglycerin bioactivation and superoxide formation by aldehyde dehydrogenase-2. J Biol Chem. 284: 19878-86 (2009)
29. R. Neubauer A. Neubauer, G. Wölkart, C. Schwarzenegger, B. Lang, K. Schmidt, M. Russwurm, D. Koesling, A. C. Gorren, A. Schrammel and B. Mayer. Potent inhibition of aldehyde dehydrogenase-2 by diphenyleneiodonium: focus on nitroglycerin bioactivation. Mol Pharmacol. 84: 407–414 (2013)
30. Y. Zhao, P. E. Brandish, M. DiValentin, J. P. M. Schelvis, G. T. Babcock and M. A. Marletta. Inhibition of soluble guanylate cyclase by ODQ. Biochemistry. 39: 10848-54 (2000)
31. M. V. Wenzl, M. Beretta, M. Griesberger, M. Russwurm, D. Koesling, K. Schmidt, B. Mayer and A. C. Gorren. Site-directed mutagenesis of aldehyde dehydrogenase-2 suggests three distinct pathways of nitroglycerin biotransformation. Mol Pharmacol. 80: 258–266 (2011)
32. J. A. Carvajal, A. M. Germain, J. P. Huidobro-Toro and C. P. Weiner. Molecular mechanism of cGMP-mediated smooth muscle relaxation. J Cell Physiol. 184: 409-420 (2000)
33. S. A. Waldman and F. Murad. Biochemical mechanisms underlying vascular smooth muscle relaxation: the guanylate cyclase-cyclic GMP system. J Cardiovasc Pharmacol. 12: 115-8 (1988)
34. U. Hink, A. Daiber, N. Kayhan, J. Trischler, C. Kraatz, M. Oelze, H. Mollnau, P. Wenzel, C. F. Vahl, K. Ki Ho, H. Weiner and T. Munzel. Oxidative inhibition of mitochondrial aldehyde dehydrogenase promotes nitroglycerin tolerance in human blood vessels. J Am Coll Cardiol. Elsevier. 50: 2226-2232 (2007)

35. I. S. De La Lande, T. Philp, I. Stafford and J. D. Horowitz. Lack of inhibition of glyceryl trinitrate by diphenyleneiodonium in bovine coronary artery. Eur J Pharmacol. 314: 347-350 (1996)
36. M. G. Bonini, K. Stadler, S. De Oliveira Silva, J. Corbett, M. Doer, J. Petranka, D. C. Fernandes, L. Y. Tanaka,D. Duma, F.R. M. Laurindo and R. P. Mason. Constitutive nitric oxide synthase activation is a significant route for nitroglycerin-mediated vasodilation. Proc Natl Acad Sci U.S.A. 105: 8569–8574 (2008)
37. L. J. Ignarro and P. J. Kadowitz. The Pharmacological and Physiological Role of Cyclic GMP in Vascular Smooth Muscle Relaxation. Annual Review of Pharmacology and Toxicology. 25: 171-191 (1985)
38. M. E. Soto, E. Soria-Castro, V. Guarner Lans, E. Muruato Ontiveros, B. I. Hernandez Mejia, H. J. Martinez Hernandez, R. Barragan Garcia, V. Herrera and I. Perez-Torres. Analysis of Oxidative Stress Enzymes and Structural and Functional Proteins on Human Aortic Tissue from Different Aortopathies. Oxid Med Cell Longev. 760694 (2014)
39. N. B. Surmeli and M. A. Marletta. Insight into the rescue of oxidized soluble guanylate cyclase by the activator cinaciguat. Chembiochem. 13: 977-981 (2012)